

T. Jin<sup>1</sup>, and S-G. Kim<sup>1</sup>

<sup>1</sup>Neuroimaging laboratory, Department of Radiology, University of Pittsburgh, Pittsburgh, PA, United States

**Introduction** The chemical exchange saturation transfer (CEST) approach, based on the hydroxyl-water proton exchange, can provide valuable information on the concentration of glycogen, glycosaminoglycans, and myo-inositol [1-3], etc. Compared to the well-studied amide-water proton exchange for which a long and low-power irradiation pulse is generally adopted, the faster hydroxyl-water proton exchange suggests that a higher irradiation pulse power would be necessary to optimize the chemical exchange (CE) contrast. Unfortunately, given the smaller chemical shift between the hydroxyl and water protons, this would also lead to a larger direct water saturation effect. Recently, it was reported that a similar CE contrast can be obtained with a frequency offset-dependent spin-locking (SL) approach which minimizes the contamination of the direct water saturation effect [4]. In this work, we evaluated the hydroxyl-water CE contrast with the CEST and SL approaches.

**Theoretical background** In a CEST experiment, the signal intensity as a function of irradiation pulse frequency  $\Omega$  is referred to as the Z-spectrum. The chemical exchange contrast is usually measured by  $MTR_{asym}(\Omega) = MTR(-\Omega) - MTR(\Omega) = [M_{CEST}(-\Omega) - M_{CEST}(\Omega)]/M_0$ . Assuming a two-site exchange and that the populations of two exchanging proton pools are highly unequal—*i. e.*  $p_A \gg p_B$  ( $p_A + p_B = 1$ ) where  $p_A$  and  $p_B$  are the relative populations of the water and labile proton, respectively—Trott and Palmer recently reported for SL experiments that the spin-lattice relaxation rate in the rotating frame  $R_{1p}$  ( $= 1/T_{1p}$ ) can be expressed as [5]:

$$R_{1p} = R_1 \cos^2 \theta + (R_2 + R_{ex}) \sin^2 \theta, \quad \text{where } R_{ex} = \frac{p_B \cdot \delta^2 \cdot k}{(\delta - \Omega)^2 + \omega_1^2 + k^2} \quad (1)$$

where  $R_1$  is the longitudinal relaxation rate of water,  $R_2$  is the intrinsic water transverse relaxation rate in the absence of chemical exchange,  $\omega_1$  ( $= \gamma B_1/2\pi$ ) is the Rabi frequency of the SL pulse,  $\theta = \arctan(\omega_1/\Omega)$  is the angle between the effective  $B_1$  field and  $B_0$ , and  $\delta$  and  $k$  are the chemical shift and exchange rate between the labile protons and water, respectively. To study the CE effect, SL relaxation dispersion experiments can be performed at the water resonance ( $\Omega = 0$ ) as a function of  $\omega_1$  [4]. SL experiments can also be performed as a function of offset frequency ( $\Omega$ ), similar to a CEST Z-spectrum. The magnetization at a spin-locking time (TSL), with repetition time  $\rightarrow \infty$ , is [4]:

$$\frac{M_{SL}(\Omega)}{M_0} = \frac{(R_2 + R_{ex}) \sin^2 \theta}{(R_2 + R_{ex}) \sin^2 \theta + R_1 \cos^2 \theta} \cdot \exp\left[-[(R_2 + R_{ex}) \sin^2 \theta + R_1 \cos^2 \theta] \cdot TSL\right] + \frac{R_1 \cos^2 \theta}{(R_2 + R_{ex}) \sin^2 \theta + R_1 \cos^2 \theta} \quad (2)$$

Similar to the  $MTR_{asym}$  parameter in CEST studies, an asymmetry parameter can be defined as the normalized differential signal acquired from opposite frequency offsets with respect to water:  $SLR_{asym}(\Omega) = SLR(-\Omega) - SLR(\Omega) = [M_{SL}(-\Omega) - M_{SL}(\Omega)]/M_0$ .

**Methods** MRI experiments were performed on a 9.4-T magnet with a 38-mm inner diameter volume coil. 100mM Glycogen (Gly) and 50mM Myo-inositol (mIns) were dissolved in PBS (pH = 7.4) and measured at room temperature. EPI images were acquired after either an SL preparation pulse with duration TSL or a CEST irradiation pulse with duration  $T_{sat}$ , and the imaging parameters were: field of view =  $24 \times 24$  mm<sup>2</sup>, matrix size =  $64 \times 64$ , slice thickness = 5 mm, and the repetition time was 18 s. For CEST Z-spectra and  $\Omega$ -dependent SL spectra, images were collected within  $\pm 10$  ppm of the water resonance, using a 5-s SL or CEST irradiation pulse with  $\omega_1 = 100$  Hz. To calculate  $SLR_{asym}$  and  $MTR_{asym}$ , control images were acquired at the offset frequencies of  $\pm 300$  ppm.  $SLR_{asym}$  and  $MTR_{asym}$  were also measured at 1 ppm with varied  $\omega_1$  and TSL or  $T_{sat}$ . Finally, on-resonance  $R_{1p}$  dispersion was measured in the range of  $\omega_1$  of 125 to 2828 Hz.  $p_B$ ,  $\delta$ ,  $k$ , and  $R_2$  were obtained by fitting the on-resonance  $R_{1p}$  dispersion data to Eq. (1). From these fitted results,  $SLR_{asym}$  as a function of TSL and  $\omega_1$  were simulated for  $\Omega = 1$  ppm using Eq. (2).

**Results and discussions** For Gly and mIns,  $SLR_{asym}$  and  $MTR_{asym}$  lineshapes that were measured with  $\omega_1 = 100$  Hz were similar, with  $MTR_{asym}$  being slightly smaller (Fig. A). The peak occurred at 1 ppm (400 Hz at 9.4 T) for mIns and 0.8 ppm for Gly. The difference between  $SLR_{asym}$  and  $MTR_{asym}$  at 1 ppm increases with  $\omega_1$ , as shown in Fig. B for the Gly sample (not shown for mIns). This is because CEST studies are susceptible to the direct water saturation effect, which increases with the saturation pulse power. With increasing  $\omega_1$ , the peak of  $SLR_{asym}$  and  $MTR_{asym}$  shifted to a smaller TSL or  $T_{sat}$ , and the maximum contrast occurred at  $\omega_1 = 200$  Hz and  $TSL \approx 1.2$  s. Both mIns and Gly samples showed large on-resonance  $R_{1p}$  dispersion (Fig. C). Fitting to Eq. [1] gave  $p_B = 0.003$  and 0.002,  $\delta = 370$  and 400 Hz (2323 and 2513 rad/s),  $k = 1250$  and 1980 s<sup>-1</sup>, and  $R_2 = 0.4$  and 1.15 s<sup>-1</sup> for the mIns and Gly samples, respectively.  $k/\delta = 0.54$  and 0.79 for mIns and Gly indicates that both hydroxyl-water proton exchanges were close to the intermediate exchange regime.

Using the fitted results of mIns and a measured  $R_1$  of 0.35 s<sup>-1</sup>, the  $SLR_{asym}$  that was simulated from Eq. (2) (lines, Fig. D) matched very well with the experimental data (symbols, Fig. D), indicating that SL data can be explained well with the asymmetric population model [5]. For mIns, the peak of  $SLR_{asym}$  occurred at  $\omega_1 = 141$  Hz and  $TSL \approx 2$  s. The observed shift of  $SLR_{asym}$  peak is different with the general conception from previous slow chemical exchange studies, in that the CE contrast was maximized at the steady state with a long saturation pulse. Using the fitted data of mIns, with  $\omega_1 = 141$  Hz,  $R_{ex} = 8.56$  s<sup>-1</sup> at  $\Omega = 1$  ppm and 0.73 s<sup>-1</sup> at  $\Omega = -1$  ppm. Although the hydroxyl resonance frequency was at  $\Omega = 1$  ppm (with respect to water), the non-zero  $R_{ex}$  at  $\Omega = -1$  ppm caused by exchange broadening reduced the  $SLR_{asym}$  at long TSL values. The shift of the  $SLR_{asym}$  peak to a shorter TSL was dependent on the metabolite concentrations  $p_B$ ,  $T_1$ , and  $T_2$  of water. For example, with a lower  $p_B$ , a higher  $\omega_1$  is necessary to see the shift in  $SLR_{asym}$  peaks (simulation data not shown). In summary, our results show that the SL approach is a good choice for the study of water-hydroxyl chemical exchange effects.

**Acknowledgments:** This work is supported by NIH grants EB008717, EB003324, EB003375, and NS44589.

**References:** [1]. Van Zijl PCM et al., *PNAS* (2007). [2]. Ling W et al., *PNAS* (2008). [3]. Haris M et al., *NeuroImage* in press. [4]. Jin T et al., *MRM* in press. [5] Trott O et al., *JMR* (2002).

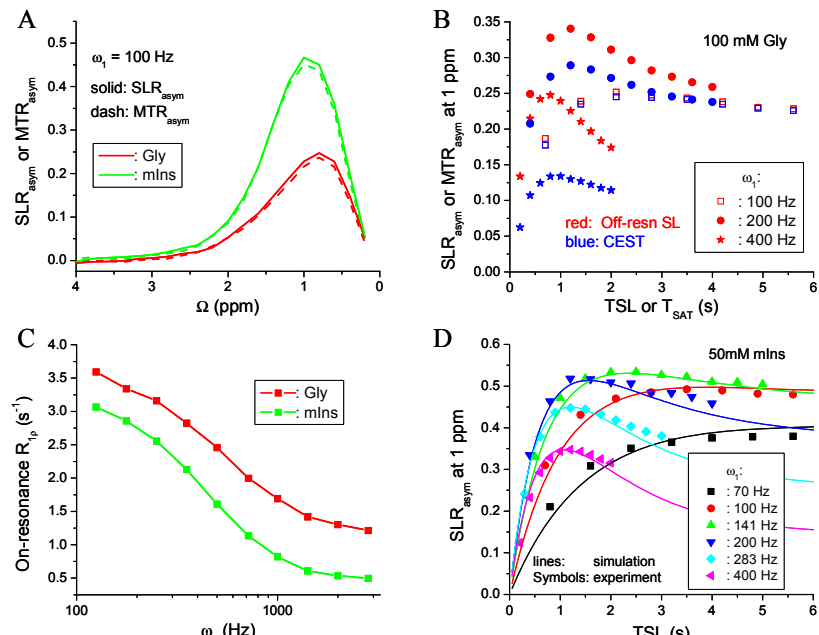


**Figure (A)**  $SLR_{asym}$  and  $MTR_{asym}$  lineshapes, measured with  $\omega_1 = 100$  Hz, are quite similar. **(B)** For Gly, the difference in  $SLR_{asym}$  and  $MTR_{asym}$  measured at 1 ppm increases with  $\omega_1$ . **(C)** Both Gly and mIns samples show large on-resonance  $R_{1p}$  dispersion. **(D)** Experimental  $SLR_{asym}$  data for mIns for varied TSL and  $\omega_1$  values match well with the simulated results.